PROCEEDINGS OF SPIE

SPIEDigitalLibrary.org/conference-proceedings-of-spie

MSE spectrograph optical design: a novel pupil slicing technique

P. Spanò

P. Spanò, "MSE spectrograph optical design: a novel pupil slicing technique," Proc. SPIE 9147, Ground-based and Airborne Instrumentation for Astronomy V, 91474D (8 July 2014); doi: 10.1117/12.2056894

Event: SPIE Astronomical Telescopes + Instrumentation, 2014, Montréal, Quebec, Canada

MSE spectrograph optical design: a novel pupil slicing technique

P. Spanò *[a]

[a]National Research Council of Canada - HIA, 5071 W. Saanich Rd., Victoria, BC, V9E2E7, Canada

ABSTRACT

The Maunakea Spectroscopic Explorer shall be mainly devoted to perform deep, wide-field, spectroscopic surveys at spectral resolutions from ~2'000 to ~20'000, at visible and near-infrared wavelengths. Simultaneous spectral coverage at low resolution is required, while at high resolution only selected windows can be covered. Moreover, very high multiplexing (3200 objects) must be obtained at low resolution. At higher resolutions a decreased number of objects (~800) can be observed. To meet such high demanding requirements, a fiber-fed multi-object spectrograph concept has been designed by pupil-slicing the collimated beam, followed by multiple dispersive and camera optics. Different resolution modes are obtained by introducing anamorphic lenslets in front of the fiber arrays. The spectrograph is able to switch between three resolution modes (2000, 6500, 20000) by removing the anamorphic lenses and exchanging gratings. Camera lenses are fixed in place to increase stability. To enhance throughput, VPH first-order gratings has been preferred over echelle gratings. Moreover, throughput is kept high over all wavelength ranges by splitting light into more arms by dichroic beamsplitters and optimizing efficiency for each channel by proper selection of glass materials, coatings, and grating parameters.

Keywords: high-resolution spectrograph, pupil-slicing, VPH grating, MSE, CFHT, multi-object spectroscopy.

1. INTRODUCTION

Maunakea Spectroscopic Explorer (MSE, formerly ngCFHT) is a proposal to replace the current 3.6m CFHT with a dedicated 10-m telescope for spectroscopic surveys. The new facility would be installed on the existing telescope pier and equipped with a wide-field (1.5 deg^2), massively multiplexed (N_{fiber} = 800-3200) fibre spectrograph. A preliminary study has been performed in the last few years to address both scientific drivers and technical feasibility[1,2].

MSE shall be mainly devoted to perform deep, wide-field, spectroscopic surveys at spectral resolution from ~2,000 to ~20,000, at visible and near-infrared wavelengths. Main parameters are given in Table 1. At low resolution (R~2'000), simultaneous coverage must be complete at both visible and near-infrared wavelengths coupled to the highest multiplexing. At higher resolutions spectral coverage and multiplexing can be smaller at expenses of higher resolution. The ideal spectrograph should be able to switch between different resolutions by a small number of mechanisms, moving few elements in order to increase instrument stability and reliability.

Table 1. MSE main parameters.

Telescope Diameter	10 m	
Field of view diameter	1.5 deg^2	hexagonal
Fiber diameter	0.9 arcsec	goal: 1.2
Wavelengths	370 – 1300 nm	goal: 350-1300
Spectral resolution	~2,000 – 20,000	goal: ~30,000
Simultaneous coverage	>λ/7	
Number of objects	800 – 3200	3200 only at R 2000
Total throughput	>20%	over 90% of all wavelengths

* paolo.spano@nrc-cnrc.gc.ca; phone 1 250 363-0017

Ground-based and Airborne Instrumentation for Astronomy V, edited by
Suzanne K. Ramsay, Ian S. McLean, Hideki Takami, Proc. of SPIE Vol. 9147,
91474D · © 2014 SPIE · CCC code: 0277-786X/14/$18 · doi: 10.1117/12.2056894

Table 2. Comparison of some wide-field MOS and IFU facilities, including telescope diameter, spectral coverage, resolution, multiplexing, fiber size, beam size, and overall throughput from telescope to detected photons.

Instrument	D_{tel} (m)	λλ (μm)	R_{max}	N_{MOS}	Fiber (")	Beam (mm)	Grating type	ε_{max} (tot)
2dF	3.9	0.37-1.0	17,000	400	2.1	190	VPH	5%
FLAMES	8.2	0.37-0.95	25,000	130	1.2	180	Echelle	9%
Hectochelle	6.5	0.38-0.90	40,000	240	1.5	260	Echelle	10%
FMOS	8.2	0.9-1.8	2,200	400	1.2	150	Grat.,VPH	10%
HERMES	3.9	4 windows	28,000	400	2.0	195	VPH	10%
APOGEE	2.5	1.5-1.7	22,500	300	2.0	280	VPH	16%
PFS	8.2	0.37-1.3	4,500	2400	1.1	280	VPH	18%
VIRUS	10	0.35-0.55	700	33600	1.5	125	VPH	18%

High-throughput, high-multiplexing (hundreds or thousands of objects) high-resolution (resolving power above 10'000) spectrographs on large telescopes (8-10m diameter) are generally very large and expensive systems. Recently, high-multiplexing has been achieved by replicating many spectrograph units, as in MUSE and VIRUS, two integral-field spectrographs. Table 2 shows a list of spectroscopic facilities in operation or under development. Comparison with the MSE requirements shows that MSE require larger spectrograph etendue and multiplexing with respect existing capabilities. So far, high-resolution spectroscopy on 6-10 meter class telescopes has been achieved by echelle spectrographs only (with very steep blaze angles, up to 76 degrees), with relatively low efficiencies. Moreover, increasing multiplexing by a large factor adds complexity to echelle spectrographs. VPH gratings offer higher peak efficiencies than echelle gratings. However, keeping their spectral coverage large requires Bragg angles smaller than 30-35 degrees, thus delivering smaller resolutions with respect the echelle spectrographs of the same size. Higher Bragg angle grating (Dickson VPHs) must be ruled out for MSE, because of their narrow spectral coverage. Indeed, two spectrographs in Table 2 adopted large angle VPH gratings, namely APOGEE[3] and HERMES[4], at expense of their spectral coverage.

2. A NEW PUPIL SLICING TECHNIQUE

We propose here a novel pupil slicing technique which offers good image quality and high throughput while keeping the size of dispersers relatively small. Inside the spectrograph optics light exiting circular fibers is processed to reduce the effective size of the projected slit image, thus increasing resolution. Figure 1 shows how images and pupils are modified along the optical path.

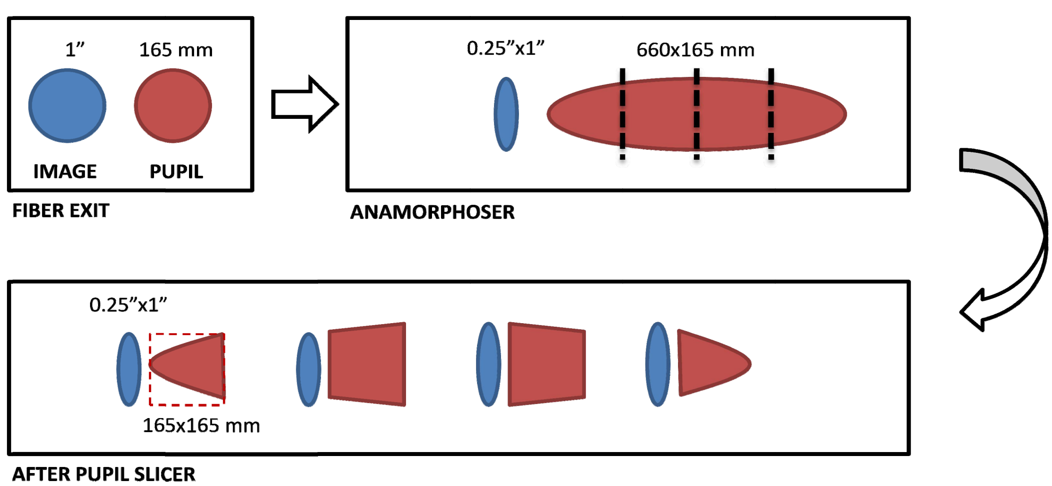

Figure 1. High-resolution is achieved by slicing the pupil (slicing factor 4).

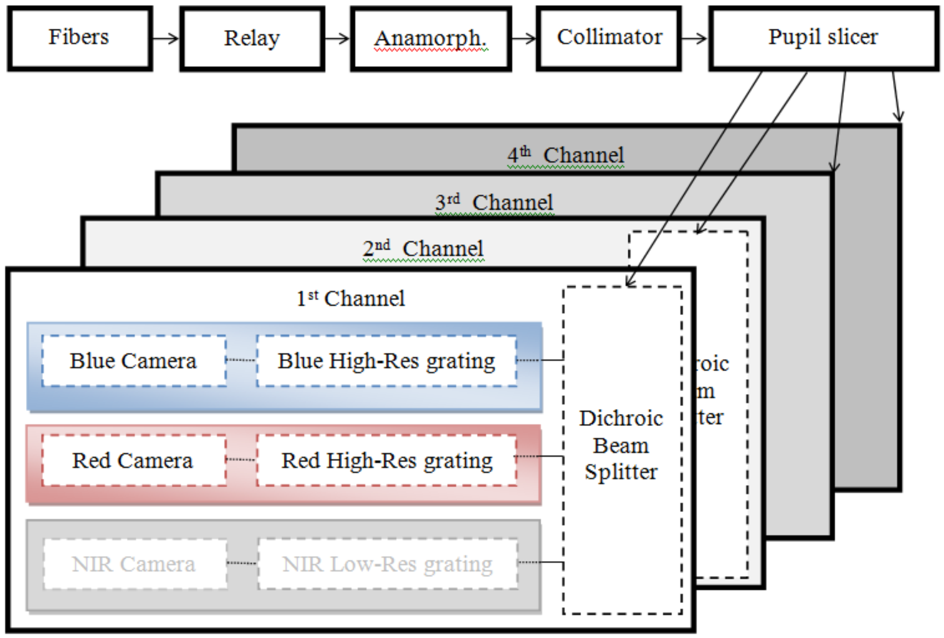

Figure 2. In high-resolution mode, after slicing the pupil, light is processed by more channels, one per sub-pupil.

At the entrance of the spectrograph each fiber (1 arcsec) will project a circular beam (round red pupil). By mean of an anamorphoser, the collimated beam is elongated by a factor K in the horizontal direction. At the same time, the image size is effectively reduced by a factor 1/K in the same horizontal direction. The elongated pupil is then sliced K times, so that each sub-pupil will be almost square and will produce a compressed image. As a result, light collected by each fiber will be split into K channels and collected by K detectors. The spectrum of a single target will need to be recovered by adding these spectra together during data reduction.

This pupil slicing method has been applied to design the MSE high-resolution spectrograph. Figure 2 gives a functional sketch of its design. Light from fiber arrays is reimaged onto the anamorphoser (made by cylindrical optics in our case). The light is then collimated and split into four identical channels (K=4 was selected as a trade-off between resolution and complexity) by a common pupil slicer placed near the exit pupil of the collimator. Each channel consists of a dichroic tree to separate wavelengths into arms (two visible arms, blue and red; a third near-infrared arm is not used in the high-resolution mode and is shaded in the figure). In each arm VPH gratings will disperse light and optimized cameras will focus spectra onto detectors.

The large collimation optics, however, can accept light coming from K separate fiber arrays instead of only one, as shown in Figure 3. Each fiber array will project its own circular pupil. These K circular pupils can be accommodated inside the same collimator exit pupil required for the high-resolution mode. The anamorphoser must be replaced by a beam combiner (e.g., a prism-plate) to direct the light from different fiber arrays inside the different channels. Each fiber of the array will feed a single channel of the spectrograph optics. The effective slit width is larger than in the pupil-slicing mode, thus providing a lower resolution (approximately ~1/K of the high resolution), but at the same time more fibers can be simultaneous observer, gaining a factor K in multiplexing. Figure 4 shows how this low-resolution (LR) mode has been implemented on MSE.

Two exchange mechanisms are required to switch between the two resolution modes. These mechanisms, however, enable two other additional resolution modes (R~6500). Indeed, by combining the anamorphoser with the LR gratings we can have full spectral coverage for 800 objects, while coupling the prism-plate with the HR gratings highest multiplexing (3200) can be achieved over selected spectral regions. These observing modes are described in the next section.

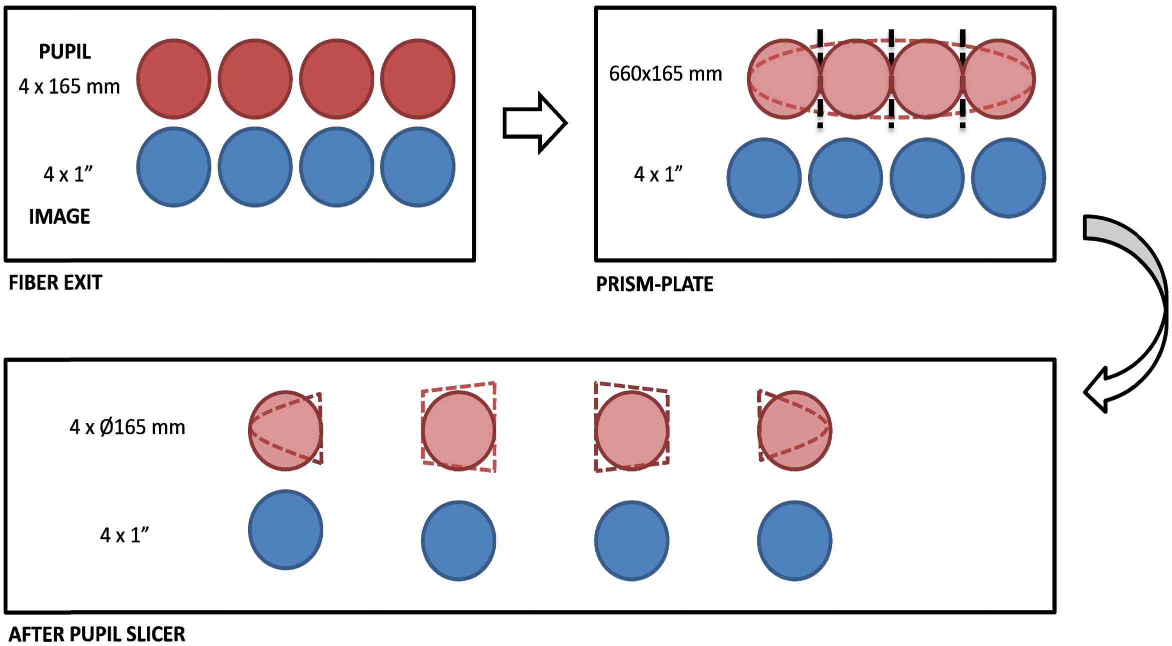

Figure 3. In low-resolution mode many pupils will overfull the elongated pupil of the high-resolution mode.

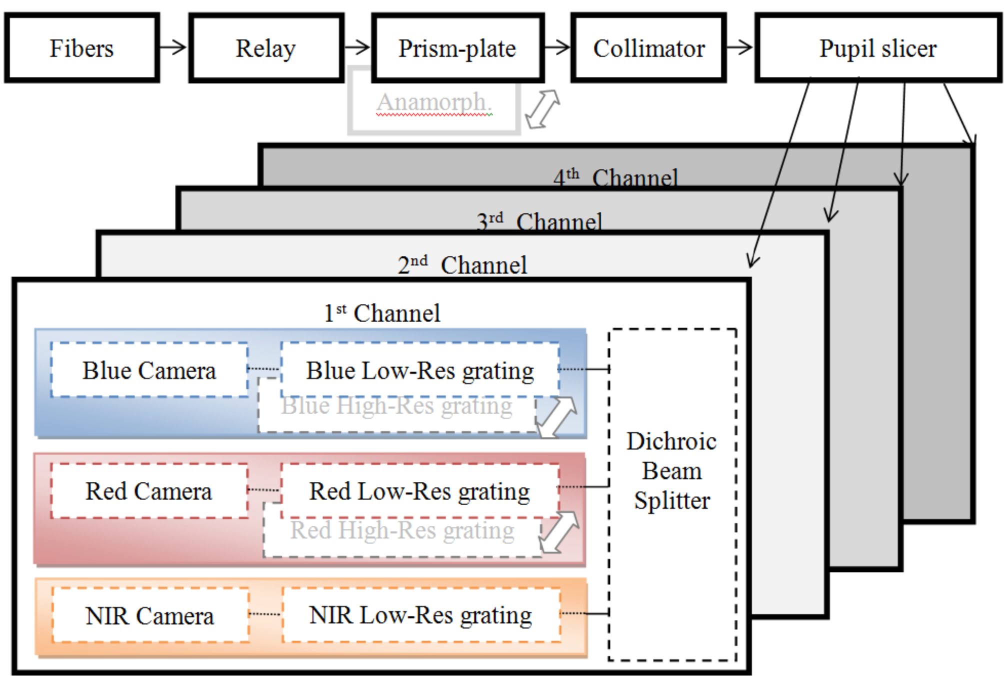

Figure 4. Low-resolution mode implementation of MSE.

3. THE MSE HIGH-RESOLUTION SPECTROGRAPH

In order to implement the two functional schemes into a real optical design many choices must be done about the first order parameters of the different sub-systems sketched in Figures 2 and 4. For each sub-system we need to define the f-ratio, beam size, field size, wavelength range, and so on. Optical interfaces between sub-systems have been provisionally defined, to simplify the design stage. This modular approach allows to optimize or to change some of the sub-systems, if required, without the need to fully redesign the whole optical train.

One of the first choices to be made is the selection of the disperser type. Indeed, only two different types of gratings have been used for high-resolution astronomical spectrographs, namely echelle gratings, mostly used in reflection to enhance their throughput, and volume-phase holographic (VPH) gratings, used in transmission.

Echelle gratings can deliver very high-resolving power by mean of steep blaze angles. The steepest angle used on existing astronomical spectrographs is 76 degrees (R-4). Even higher blaze angles (up to 81 degrees, or R-6) have been ruled, for example for the Subaru IRD[5] spectrograph, but the main limitation is given by the highly variable spectral sampling across each diffraction order. While providing very high resolving powers, these gratings are used at high diffraction orders, where the free spectral range is relatively small. Then, to recover larger wavelength ranges, many orders must be measured with multiple observations with order-sorting narrowband filters, or by cross-dispersing different orders in the spatial direction. In the former case higher multiplexing can be reached at cost of a quite limited simultaneous spectral coverage. Then, many observations with different filter and/or gratings are required to retrieve the full spectrum. In the latter case, cross-dispersed echelle spectrographs overcome the limitation of small simultaneous spectral coverage at expenses of multiplexing.

VPH gratings behave very well in the first order providing very high peak efficiencies over a wide bandwidth. However, bandwidth is a strong function of the Bragg angle. Different authors[6,7] have shown there is an optimal range of Bragg angles between ~15 and ~35 degrees for which efficiency peaks at ~90% and bandwidth is quite large. For higher angles, peak efficiency drops and then rises again for a smaller range of angles (“Dickson” gratings). Those devices, while delivering high peak efficiency (~90%), exhibit relatively narrow bandwidths, making them less attractive for a wideband spectrograph as MSE.

MSE asks for both HR and LR gratings, to optimize efficiency and simultaneous coverage. Our goal is to select two basic angles, one for the HR gratings and another one for the LR gratings, which simultaneously maximize resolving power, peak efficiency and bandwidth for both modes. Our best trade-off was a HR grating angle of 37 deg (corresponding to a Bragg angle~24 deg for n=1.5 medium) with an estimated diffraction efficiency peak of 90%, and a LR grating angle of 14 deg (see Figure 5). Once telescope diameter, fiber aperture, grating angle, and resolution are fixed, the only free parameter is the collimated beam size. This will give the size of our elongated pupil. Of course, without the pupil slicing technique, very large gratings and very fast camera optics should be required to design the spectrograph. If the collimated beam is ~65cm in the elongated direction, by selecting a 4X pupil slicing factor beam size on gratings is reduced to ~16 cm only. Once sub-pupil size is defined, camera optics parameters can be defined, too. The trade-off is between spectral sampling, spatial sampling, multiplexing and simultaneous coverage. A reasonable sampling of spectra at both HR and LR modes must be defined. Multiplexing will be further controlled by the required minimum gap between adjacent spectra to allow proper data extraction and minimal cross-contamination.

A summary of the main characteristic of the final spectrograph design is given in Table 3. Four different observing modes have been defined:

- **Low-Resolution (LR)**: low-resolution gratings and prism-plate are selected. In this way up to 3200 fibers can be fed into the spectrograph, 800 per channel. Full spectral coverage is obtained at R~2’000, covering all visible and NIR wavelengths, simultaneously.

- **Medium-Resolution Full-Coverage (MR-FC)**: still keeping low-resolution gratings in place, the prism-plate is exchanged with the anamorphoser, thus selecting a subsample of 800 fibers to be observed at higher resolution (R~6’500). The spectral coverage is still complete in the visible, but NIR wavelengths are undersampled. Each fiber will produce four spectra, to be added by SW.

- **Medium-Resolution High-Multiplexing (MR-HM)**: another way to obtain an intermediate resolution (~6’500) for all 3200 fibers is to keep the prism-plate in place and insert the HR gratings. Spectral coverage is reduced to two wavelength ~λ/7 windows. Different gratings will be available to select the central wavelength of those two windows. Also near-infrared wavelengths can be observed, but at a lower resolution (the same of the LR mode).

- **High-Resolution (HR)**: when high-resolution is required, high-resolution gratings must be coupled to the anamorphoser, then delivering R~20'000 in the visible range. Due to limited detector size, only two ~λ/7 wavelength windows will be observed simultaneously, placed around two selectable central wavelengths. NIR wavelengths are not measured due to undersampling in the NIR arms. The multiplexing factor is 800.

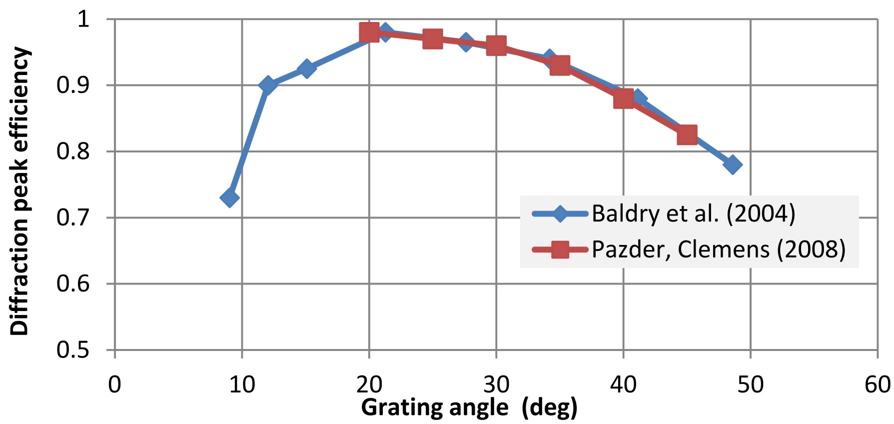

Figure 5. First-order un-polarized VPH diffraction efficiency based on rigorous-coupled wave analysis (RCWA).

Table 3. Main MSE spectrograph characteristics.

Parameter	Value	Note
Fiber diameter	0.9 arcsec	*(155 um at F/3.5)*
Resolving power	2000 6500 20000	*LR mode* *MR-FC & MR-HM modes* *HR mode*
Spectral bandwidth	370 – 1300 nm	
Simultaneous coverage	Full (370 – 1300 nm) Full (370 – 850 nm) 2 selectable λ/7 windows	*LR mode* *MR-FC mode* *HR & MR-HM modes*
Spectral Sampling	10 pixel 4.5 pixel 2.5 pixel	*Visible arms, LR & MR-HM modes* *NIR arm, LR & MR-HM modes* *Visible arms, HR & MR-FC modes*
Interspectra separation	7 pixel 3 pixel	*Visible arms* *NIR arms*
Number of fibers	1800 ± 10% 450 ± 10%	*LR & MR-HM modes* *HR & MR-FC modes*
Detectors	9kx9k, 10um CCD (8X) 4kx4k, 15um FPA (4X)	*Visible arms* *NIR arm*
Efficiency	50% ± 5% (at peak)	*Spectrograph optics + detectors*

4. OPTICAL DESIGN

Figure 6 shows the layout of the different components of the spectrograph unit. Fibers at the entrance will be processed by a set of identical relay optics. At the intermediate focal plane, anamorphosers or prism-plates can be inserted to switch between different observing modes. The light is then collimated by a mirror, and aberrations corrected by two lenses. The collimated beam is finally split into four identical channels by the pupil slicer. Each channel will consist of two dichroic beam-splitters, VPH gratings, and three optimized refractive cameras. Many fiber bundles will populate the long entrance slit of the spectrograph collimator with different light patterns, according to the selected observing mode. In the HR and MR-FC case, the anamorphoser will enlarge the pupil in the main dispersion direction (lying in the plane of the figure), thus feeding the different channels with light coming from the same fiber array. Each fiber will project 12 different spectra: 4 in the blue detectors, 4 in the red ones, and 4 in the NIR ones (4 spatial split x 3 wavelength split). The same wavelength will be split into four detectors, and spectra will be reconstructed by SW. In the LR and MR-HM case, the prism-plate will send the light coming from four adjacent fiber arrays into the four channels (as like as feeding four separate spectrographs). Each fiber will project only 3 different spectra (wavelength split only). In this case, no reconstruction is required to recombine light of the same wavelength. The modularity of this design allows replicating many sub-system components.

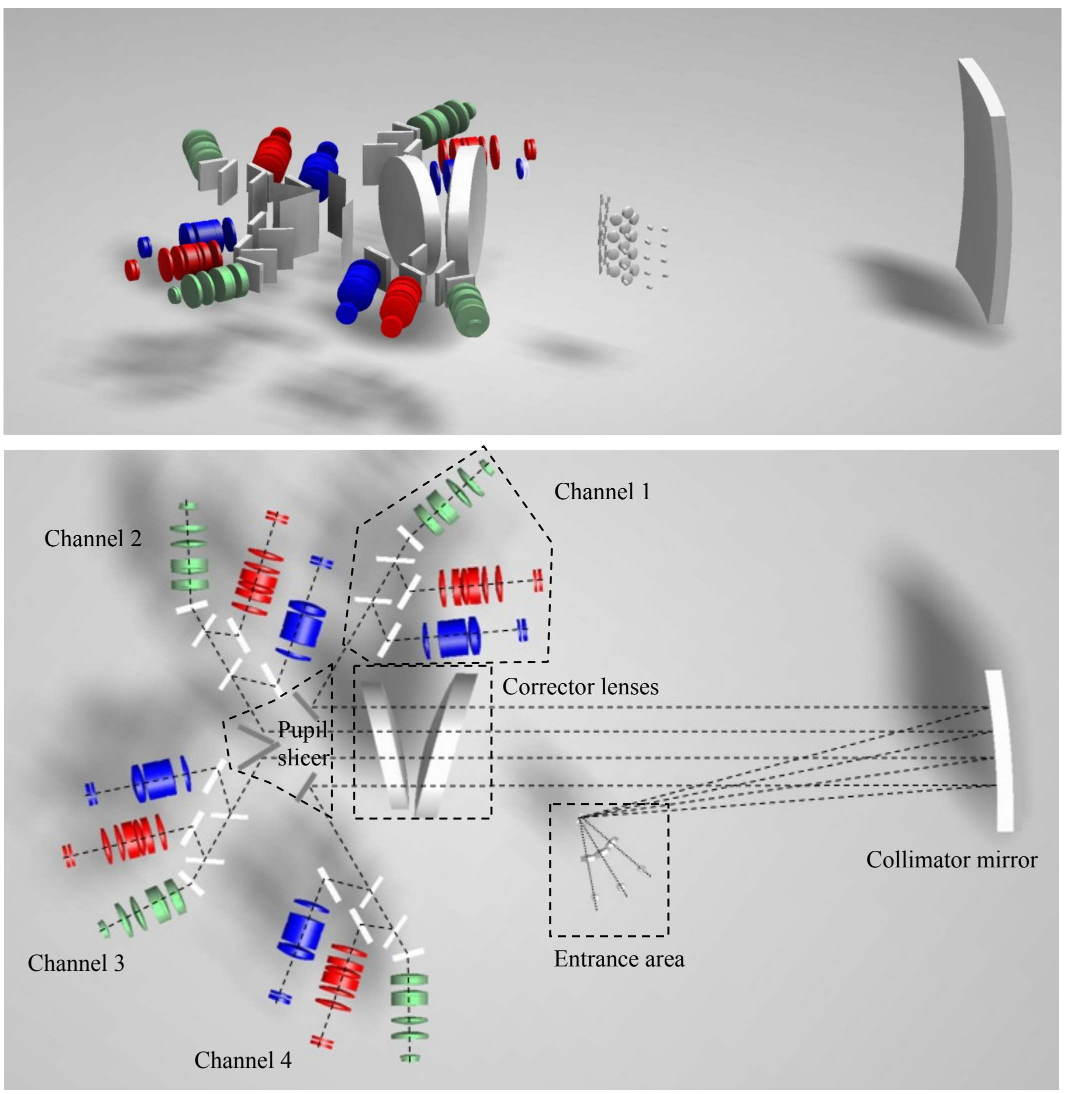

Figure 6. Lateral and top views of the spectrograph optics.

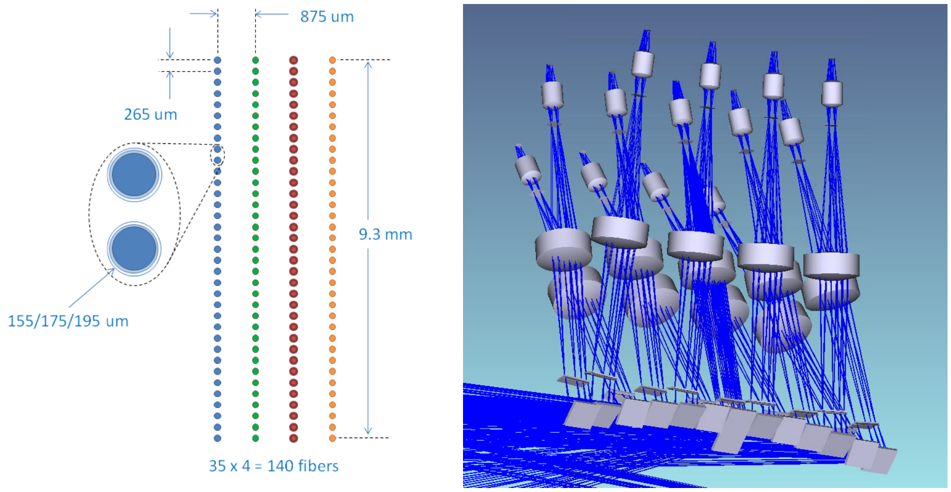

Figure 7. Sketch of a fiber array at the exit of each bundle (left) and the full relay optics (right).

Fibers from the telescope focal plane will carry light at F/3.5, in order to minimize focal ratio degradation. They will be routed on bundles, each one containing 140 fibers, aligned into four different columns, as shown in the Figure 7. The full set of fibers is split into 13 identical bundles (13x140 = 1820), each one coupled to relay optics. To keep the optical and mechanical interfaces simple, all fibers will be coaxial and perpendicular to a flat surface. This choice opens to both post polishing of the assembled bundle, or to assembly pre-polished fibers onto a laser machined micro-hole plate.

The relay optics will adapt the F/3.5 fiber output beam into the F/16 collimator input beam. Each relay consists of two cemented triplets (CaF2 and Schott N-BaK1/N-BaK2) with very small internal losses. Each triplet incorporates an aspherical surface to improve image quality (rms spot diam. < 0.15”) and telecentric correction. Lens diameters are 30 and 70 mm. Lenses will be anti-reflection coated. Due to the very wide bandwidth, the best candidate is a SolGel/MgF2 coating, providing an average reflectivity of ~1% between 365 to 1300 nm. The overall throughput is estimated ~95% over the full band, peaked at ~97% in the visible bands. A pupil stop is placed between the two triplets, to control beam illumination patterns onto the spectrograph pupil.

A cylindrical microlens is used to introduce a 4X anamorphic magnification. The entrance surface is an aspherical cylinder and the exit surface is toroidal. This microlens can be manufactured by advanced techniques, like photolithography, resist processing or reactive ion etching. These technologies allow a very accurate shaping of the lens profile and a precise relative positioning of the front and rear surface of the lenses.

To switch from HR to LR mode, cylindrical optics will be removed and a prism plate will be inserted. The optics will project the four columns of the fiber array onto the four channels of the spectrograph. This is done by tilting the chief ray of each column into the proper sub-pupil position, by mean of TIR prisms. To prevent cross-contamination between adjacent channels, a rectangular diaphragm is inserted into the relay optics, providing room for clean beam separation (a ~1.5% small vignetting will be introduced).

The largest component of the optical train is the collimator, based onto a spherical mirror and two corrector lenses. The spherical mirror aperture is 1.5 x 1.0 m, while the two corrector lenses are off-axis portions of meniscus shaped lenses. Their clear aperture is 90-cm. One corrector lens is spherical, while the other contains an aspherical surface (~350 um departure, <4mrad slope deviation), for aberration control. Both corrector lenses can be done in fused silica (high-transmission over the whole band, high-homogeneity, available in large sizes), but enhanced-UV grade BK7 could be an option. SolGel/MgF2 coating is foreseen for the lenses. On the spherical mirror, enhanced Silver has been successfully applied in the past for large mirrors.

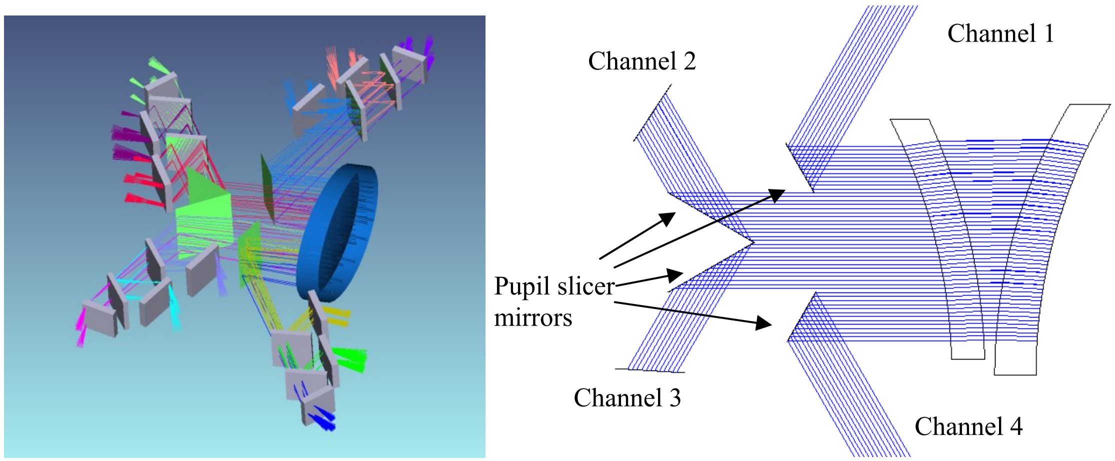

Figure 8. Pupil slicer mirror layout.

In order to slice the elongated pupil, four rectangular shape flat mirrors have been used. They are shown in Figure 8. Those mirrors are not in the pupil plane, but the beams belonging to different fibers are almost aligned in the vertical direction only, making it possible to slice the pupil far from the pupil plane. These mirrors can share the same reflective coating of the primary, but even better performances could be obtained with all-dielectric coatings, because of the much smaller size.

Different wavelengths will be separated through two dichroic beam splitters in series. The first one shall reflect shorter wavelengths (λ<525 nm) while transmitting longer wavelengths, the second will reflect below 900 nm. They work at a relatively small angle of incidence (~25 deg), to make the transition region sharper. Maximum clear aperture is about 22x28 cm, well within current manufacturing technologies. To improve performances, an exchange mechanism can be implemented, to select the best transition region for the given observing mode. Moreover, when observed wavelengths fall in a single arm, its efficiency can be maximized if dichroics are replaced by mirrors and/or a dummy window (with enhanced anti-reflection coatings). Due to the crowded area, a linear stage should be implemented, out of the plane of the layout.

As previously discussed, volume-phase holographic (VPH) gratings have been selected to provide wavelength separation at very high efficiency. Two angles, 37 and 14 degrees, have been defined for high- and low-resolution modes, respectively. Maximum substrate size is 20x20 cm, well within current state-of-the-art technologies for VPH gratings. HR gratings share an incidence angle of 37 degrees, and a bandwidth of 1/7 of the central wavelength. A 10% overlap between adjacent VPH has been added, to provide some room for merging spectra during the data reduction. Three HR gratings will be installed in the Blue arms, while the Red arms will host up to 4 different HR gratings. LR gratings shall have a 14 degree incidence angle. The LR gratings will allow simultaneous full coverage of the spectrograph bandwidth. To switch between the HR and LR modes, an exchange mechanism has been foreseen that preserve the total beam deviation between the two modes, making the camera optics fixed (Figure 9). In order to exchange from the LR to the HR gratings, by keeping fixed the total beam deviation, some additional optics must be added, in order to recover for the different beam deviation introduced by different VPH Bragg angles. In the past most of the proposed solutions were based onto prisms. However, in our design those prisms should be very large, with steep incidence angles, thus reducing the width of the grating blaze function, because the entrance prism should disperse incoming light. Here we propose the addition of a single flat mirror. The exchange mechanism should switch between the HR grating and the LR grating + mirror. This solution implies a shift of the pupil at the camera entrance, but this will not degrade performances, because the layout shall be optimized for the HR mode, and the LR mode will tolerate a smaller larger (aberrated) image size, where best image quality is not required.

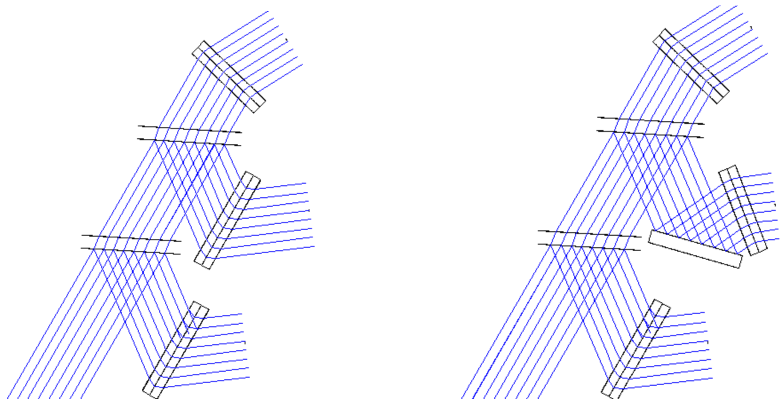

Figure 9. HR grating (left) and LR grating (right) layouts. The camera angle is not changed between the two gratings.

Three different optimized cameras will be coupled to each different arm. The wavelength splitting allow performance improvements, both in term of image quality and efficiency, because smaller chromatic corrections are required, together with enhanced anti-reflection coatings and very low internal transmission losses by proper selection of the lens glasses.

Real entrance pupils will be different at each channel in HR mode, because of the pupil slicing, and of the geometrical distortion introduced by the gratings. For some wavelength and fiber positions, some small vignetting has been introduced to save lens diameter, making easier to reach image quality performances. Optimization of the camera optics has been preliminary done without the spectrograph optics in front of its entrance pupil - referred as “stand-alone” optimization - making it easier to control optical interfaces between the two sub-systems. Anyway, better image quality can be obtained by reoptimizing lens design within the overall spectrograph design – hereafter referred as “built-in” optimization - because some chromatism can be left uncorrected.

5. SPECTROGRAPH PERFORMANCES

Spectrograph image quality has been optimized in order to deliver the highest resolving power in HR mode. For LR mode, fiber images are larger and larger aberrations can be tolerated. A provisional image quality budget has been derived as guideline during the design process of the different optical subsystems. As metrics, EE80 diameter as projected on the detector focal plane has been selected. Most of the budget is assigned to the camera optics (as usual).

Nominal RMS spot diameters are always in the 10-20 micron range, or even better. As an example of the quite uniform image quality across the detector area, EE80 diameter maps for the Red channels are shown in Figure 10. Due to some asymmetry in the optical design of each channel, there are slight differences between them.

Resolution is defined as $\lambda/\Delta\lambda$ where $\Delta\lambda$ is the Full Width Half Maximum (FWHM) of a spectral line at a given wavelength λ. For a Gaussian shaped line spread function (LSF), with standard deviation σ, we can easily convert from EE80 diameter to FWHM (=0.66 EE80D). Overall resolving power can be computed by summing up together, via RSS, the projected fiber image size, spectrograph image quality, and detector effects (flatness error, sampling, electro-optical response). Resolving powers in high-resolution and low-resolution modes are 20,000 and 2,000, respectively. This includes as-built tolerances.

All wavelengths from 370 to 1260 nm will be simultaneously observed in the LR and MR-FC modes, split into three arms. Some small overlap between adjacent wavelength ranges allow for merging of the different parts of the spectrum. In HR and MR-HM modes, only two wavelength regions per exposure can be simultaneously taken.

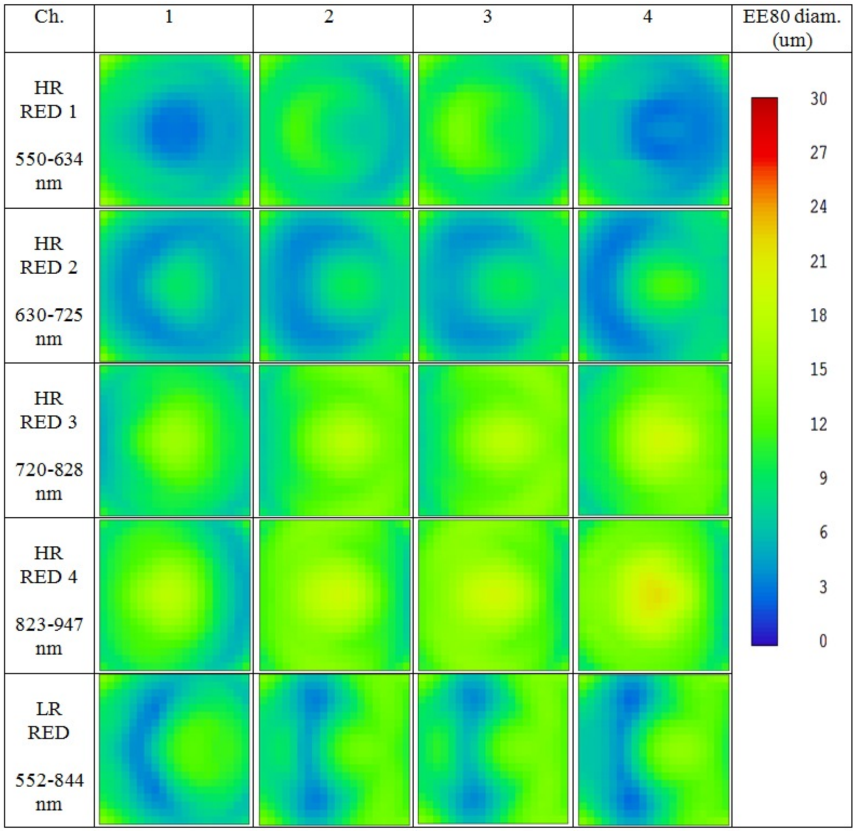

Figure 10. Spectrograph red arm EE80 diameter maps across the detector area.

In LR and MR-HM modes each fiber will project an (almost) circular shape image. Due to varying anamorphism at grating level, sampling will vary along the spectrum, slightly changing the spectral sampling. Spatial sampling will be not affected by this anamorphism.

Due to the relatively large number of pixels covered by such an image, rebinning (in the Blue and Red detectors) should be preferred, to decrease detector readout noise. Without rebinning the sampling (both spectral and spatial) will be about 10 pixel in the Blue and Red arms, and about 4.5 pixel in the NIR arm, as measured across the spectral line FWHM.

In HR and MR-FC modes, due to the additional anamorphism introduced by the anamorphoser, the spectral sampling will be decreased by a factor 4, obtaining a value of 2.5 pixel, above the Nyquist limit. All spectra will be parallel each other as projected on the detectors, almost evenly spaced. Some large gaps will be found between fiber images belonging to different fiber bundles. This empty space can be useful to add additional simultaneous calibration fibers. Due to varying incidence angles on the VPH gratings, some wavelength shift between adjacent fibers can be observed, like in long-slit spectrographs. To maximize simultaneous spectral coverage in HR mode, this effective “slit curvature” has been nulled by curving the entrance slit. Of course, this correction will work for one VPH incidence angle only. Then, in LR mode, a residual slit curvature can be seen. This has been taken into account to properly define the coverage of each LR arm.

An overall throughput budget has been built for the system, including telescope optics, wide field corrector, ADC, fiber train, and spectrograph optics, as shown in Figure 11. Spectrograph optics will have a 55% throughput between 500 and 1100 nm, falling down to 45% at 360 nm and to 50% at 1300 nm.

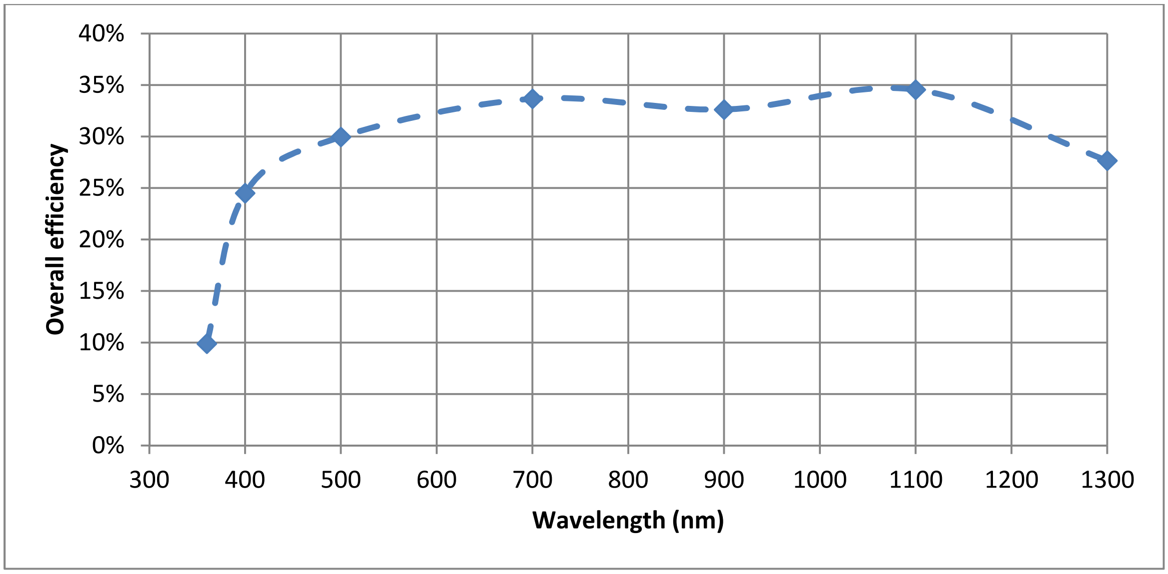

Figure 11. Overall throughput curve.

REFERENCES

[1] McConnachie, A., Murowinski, R., Salmon, D., Simons, D., Cote, P., "The Maunakea Spectroscopic Explorer: the science flowdown," Proc. SPIE 9145, (2014)

[2] Simons, D., Crampton, D., Cote, P., McConnachie, A., Szeto, K., Salmon, D., Devost, D., Murowinski, R., "Current status and future plans for the Maunakea Spectroscopic Explorer (MSE)," Proc. SPIE 9145, (2014)

[3] Wilson, J.C., Hearty, F., et al., "Performance of the Apache Point Observatory Galactic Evolution Experiment (APOGEE) high-resolution near-infrared multi-object fiber spectrograph," Proc. SPIE, 8446, 84460H (2012)

[4] Heijmans, J.A.C., Gers, L., Faught, B., "Design and development of the high-resolution spectrograph HERMES and the unique volume phase holographic gratings," Proc. SPIE 8167, 81671A (2011)

[5] Tamura, M., Suto, H., et al., "Infrared Doppler instrument for the Subaru Telescope (IRD)," Proc. SPIE 8446, 84461T (2012)

[6] Baldry, I.K., Bland-Hawthorn, J., Robertson, J.G., "Volume Phase Holographic Gratings: Polarization Properties and Diffraction Efficiency," PASP, 116, 403-414 (2004)

[7] Pazder, J., Clemens, C., "VPH grating technology for the Thirty Meter Telescope instrumentation program," Proc. SPIE, 7018, 70184U (2008)